Received: 21 May 2021 | Revised: 25 August 2021 | Accepted: 26 August 2021

DOI: 10.1111/cas.15122

Cancer Science WILEY

ORIGINAL ARTICLE

The EZH2 inhibitor tazemetostat upregulates the expression of CCL17/TARC in B-cell lymphoma and enhances T-cell recruitment

Hepei Yuan | Momoko Nishikori | Yasuyuki Otsuka | Hiroshi Arima | Toshio Kitawaki | Akifumi Takaori-Kondo

Department of Hematology/Oncology, Graduate School of Medicine, Kyoto University, Kyoto, Japan

Correspondence
Momoko Nishikori, Department of Hematology/Oncology, Graduate School of Medicine, Kyoto University. 54 Shogoin Kawahara-cho, Sakyo-ku, Kyoto, 606-8507, Japan.
Email: nishikor@kuhp.kyoto-u.ac.jp

Funding information
Japan Society for the Promotion of Science, Grant/Award Number: 15K09474 and 18K08324

Abstract

An inhibitor of the histone methyltransferase enhancer of zeste homologue 2 (EZH2), tazemetostat, has been developed for the treatment of B-cell lymphoma, but its mechanisms of action are not fully elucidated. We screened for genes targeted by tazemetostat in eleven B-cell lymphoma cell lines and found that tazemetostat significantly increased the expression of chemokine (C-C motif) ligand 17 (*CCL17*)/thymus- and activation-regulated chemokine (*TARC*) in all, which codes for a chemokine that is a hallmark of Hodgkin/Reed-Sternberg (H/RS) cells in Hodgkin lymphoma. Notably, gene set enrichment analysis demonstrated a positive correlation between the genes upregulated by tazemetostat in five follicular lymphoma (FL) cell lines and those reported to be overexpressed in H/RS cells. The *CCL17* promoter region was enriched in repressive histone modification H3K27me3, and tazemetostat induced H3K27 demethylation and activated gene transcription. CCL17 protein secretion was also induced by EZH2 inhibition, which was further enhanced by concurrent CpG stimulation. In vitro transwell migration assay demonstrated that CCL17 produced by tazemetostat-treated B cells enhanced the recruitment of T cells, which had the potential to exert antilymphoma response. Analysis of publicly available human lymphoma databases showed that *CCL17* gene expression was inversely correlated with the EZH2 activation signature and significantly paralleled the $CD4^+$ and $CD8^+$ T-cell–rich signature in FL and germinal center B-cell–like diffuse large B-cell lymphoma. Our findings indicate that tazemetostat can potentially activate antilymphoma response by upregulating *CCL17* expression in B-cell lymphoma cells and promote T-cell recruitment, which provides a rationale for its combination with immunotherapy.

KEYWORDS

B-cell lymphoma, CCL17, EZH2 inhibitor, Hodgkin lymphoma, tumor microenvironment

1 | INTRODUCTION

The histone methyltransferase enhancer of zeste homologue 2 (EZH2) is a component of the polycomb group complex and is involved in repressing gene expression through trimethylation of histone H3 on lysine 27 (H3K27). It plays roles in the regulation of development, proliferation, and differentiation of various cell types, and its aberrant activity is involved in the pathogenesis of a number of malignancies, including B-cell lymphomas.

Activating mutations in the EZH2 gene are recurrently found in follicular lymphoma (FL) and germinal center B-cell–like diffuse large B-cell lymphoma (GCB-DLBCL).[1-3] In addition, EZH2 overexpression is suggested to be involved in the pathogenesis of mantle cell lymphoma (MCL) and Burkitt lymphoma (BL).[4,5] In light of these findings, an EZH2 inhibitor, tazemetostat, has been developed for the treatment of B-cell lymphoma and is approved for the treatment of FL with EZH2-activating mutations.[6-8] However, clinical studies have shown that it is also effective to some extent for FL without EZH2 mutations and lymphomas of other histologic subtypes.[8-10] Its usefulness seems to be limited as a single agent, and it is considered necessary to understand its mechanisms of action to maximize its efficacy and application.

In this study, we aimed to elucidate the biological effects of tazemetostat that are shared among B-cell lymphomas. We screened for genes upregulated by tazemetostat in B-cell lymphoma lines and found that chemokine (C-C motif) ligand 17 (CCL17)/thymus- and activation-regulated chemokine (TARC), a chemokine that is a hallmark of Hodgkin/Reed-Sternberg (H/RS) cells in Hodgkin lymphoma (HL),[11] was significantly upregulated in all. Moreover, RNA sequencing (RNA-seq) and gene set enrichment analysis (GSEA) of five FL cell lines demonstrated a positive correlation between the genes upregulated by tazemetostat in FL cell lines and those reported to be overexpressed in H/RS cells.[12]

CCL17 is a chemokine expressed in antigen-presenting cells such as dendritic cells,[13,14] and as a ligand for CCR4, it induces trafficking of CCR4-positive T cells and facilitates the T-cell response. Although CCL17 receptor CCR4 is typically expressed on regulatory T (Treg) cells, increased CCL17 expression in lymphoma cell lines induced the recruitment of broader subsets of T cells, which had the potential to exert antilymphoma response.

According to these results, it is suggested that EZH2 inhibition in B-cell lymphomas promotes T-cell infiltration into the tumor microenvironment by upregulating CCL17. Our findings provide a rationale for the combination of an EZH2 inhibitor with immunotherapy for the treatment of B-cell lymphomas.

2 | MATERIALS AND METHODS

2.1 | Cell lines, primary lymphoma cells, and culture conditions

The following cell lines were used[15-21]: transformed FL lines FL18, FL218, FL318, FL518, FL618; a GCB-DLBCL line SU-DHL-6; activated B-cell–like (ABC)-DLBCL lines DLBCL2 and HBL-1; BL lines Raji and Daudi; an MCL line Granta-519; and HL cell lines KMH2, L428, and HDLM2. Cells were maintained in RPMI1640 medium containing 10% fetal bovine serum (FBS) and 1% penicillin/streptomycin/L-glutamine (PSG). In the experiments of tazemetostat treatment, the cell lines were cultured at 2×10^5/mL in a 24-well plate for 4 days with indicated concentrations, or 5 μM if not otherwise noted, of tazemetostat (Apexbio).

Primary lymphoma cells were collected from pleural effusion of a patient with transformed indolent B-cell lymphoma after obtaining informed consent from the patient in accordance with the ethical standards of the Helsinki Declaration and the Institutional Review Board of Kyoto University Hospital. For the culture of primary lymphoma cells, CD40 ligand (CD40L)-transfected L cells[22] irradiated with 50 Gy were first seeded at 5×10^4/mL in a 24-well plate and cultured overnight with DMEM containing 10% FBS and 1% PSG. After removing the medium, 1×10^6/mL primary lymphoma cells were cocultured with L cells in fresh RPMI1640 containing 10% FBS and 1% PSG for 3 days, with different concentrations of tazemetostat or carrier (0.1% dimethyl sulfoxide, DMSO).

2.2 | Quantitative reverse-transcription polymerase chain reaction (qRT-PCR)

Total RNA was extracted using an RNeasy Mini kit (Qiagen), and complementary DNA (cDNA) was synthesized using a SuperScript III First-Star and Synthesis system (Life Technologies). qRT-PCR was performed using TB Green Premix Ex Taq II (Takara) with primers listed in Table 1.

2.3 | Transcriptome sequencing analysis, mutation analysis, and GSEA

Total RNA was extracted from cell lines using an RNeasy Mini kit (Qiagen), and transcriptome sequencing and mutation analyses were performed at Riken Genesis (Kanagawa, Japan). Briefly, RNA-seq libraries were constructed using TruSeq Stranded mRNA Library Prep Kit (Illumina), and a multiplexed paired-end sequencing analysis was performed according to the manufacturer's instructions. Single nucleotide variant (SNV) and insertion/deletion (Indel) calls were performed using samtools (0.1.19) and filtered by QUAL (>10) and Variant Frequency (>0.3). The variants were annotated based on RefSeq (using in house program), and the genes of interest were picked up. GSEA[23] was performed on the normalized RNA-Seq expression data, and the 83 genes that were reported to be upregulated in H/RS cells microdissected from HL tissues[12] using the Broad Institute desktop application (http://software.broadinstitute.org/gsea/downloads.jsp).

2.4 | Chromatin immunoprecipitation (ChIP)-qPCR

FL318 cells were first cultured with indicated concentrations of tazemetostat or DMSO for 4 days. ChIP assay was performed in

TABLE 1 Primers used in this study

Primer name	Sequence (5′ to 3′)
qRT-PCR primers	
CCL17-F	GACCTGCACACAGAGACTCC
CCL17-R	TGTTGGGGTCCGAACAGATG
TNFRSF25-F	CTGGAGGCAGATGTTCTGGG
TNFRSF25-R	GTCCAAGGGTGACAGATGGG
IL22RA1-F	AGACACGGTCTACAGCATCG
IL22RA1-R	GTGGCTTGAGGGTAGTGTG
ID2-F	CGGATATCAGCATCCTGTCCTT
ID2-R	TCCAAGTAAGAGAACACCCTGG
BACH2-F	GAACGAGCTGCCATGTGATG
BACH2-R	GGAGCTATGTGAACGAACGC
ITGAV-F	CGCTTCTTCTCTCGGGACTC
ITGAV-R	TCACATTTGAGGACCTGCCC
ID3-F	TGGAAATCCTACAGCGCGTC
ID3-R	CTGCGTTCTGGAGGTGTCAG
PDL1-F	TGGCATTTGCTGAACGCATTT
PDL1-R	TGCAGCCAGGTCTAATTGTTTT
ChIP-qPCR primers	
CCL17 promoter-F	CTCCAGCTACAGAGAGATGAACC
CCL17 promoter-R	TCTAGAGCCCATGGCAGTGAC

accordance with a published method[24] with following modifications: FL318 cells were crosslinked with 1% formaldehyde for 5 minutes at room temperature with gentle rotation and then quenched with 0.125 M glycine. After washing, nuclei were sonicated in a Covaris S220 ultrasonicator (Covaris), and the supernatants were used for immunoprecipitation with anti-H3K27me3 monoclonal antibody (clone MABI 0323; Active Motif), anti-histone H3 antibody (MABI 0301; Active Motif), or control IgG (#5415; Cell Signaling Technology). Using the precipitated samples, the *CCL17* promoter region was analyzed by qPCR using the primers listed in Table 1.

2.5 | Knockdown of *KDM4C* by shRNA

Two different KDM4C shRNAs were cloned into the retroviral vector pSicoR-mCherry. The sequence targeted by inserting synthetic double-stranded oligonucleotides (TRCN0000022054, sense oligo, 5′-TATACTTGGATTACGAAGATTTTTCAAGAGAAAATCTTCGTAATCCAAGTATTTTTTTC-3′; antisense oligo, 5′-TCGAGAAAAAAATACTTGGATTACGAAGATTTTCTCTTGAAAAATCTTCGTAATCCAAGTATA-3′; TRCN0000235047, sense oligo, 5′-TGCCCAAGTCTTGGTATGCTATTTCAAGAGAATAGCATACCAAGACTTGGGCTTTTTTC-3′, and antisense oligo, 5′-TCGAGAAAAAAGCCCAAGTCTTGGTATGCTATTCTCTTGAAATAGCATACCAAGACTTGGGCA-3′). These vectors were cotransfected with packing plasmid mix (GE Dharmacon) into 293T-LentiX cell lines to produce lentivirus. Supernatant was collected 48 hours after transfection and concentrated by ultracentrifugation for 2 hours at 126000 *g*. Lentiviral particles were resuspended in RPMI1640 and transduced into HL cell lines HDLM2 and L428.

2.6 | Enzyme-linked immunosorbent assay (ELISA) for the detection of CCL17

Cells were cultured with the indicated concentrations of tazemetostat, with or without 1 μM CpGODN-2006 (InvivoGen) for 1 day. Their supernatants were analyzed for CCL17 using a Human CCL17/TARC Quantikine ELISA Kit (R&D Systems).

2.7 | Transwell T-cell migration assay

Peripheral blood mononuclear cells were separated from the peripheral blood of two healthy donors using a Ficoll-Paque density gradient (Cedarlane), and total T cells were collected by negative selection using MACS Cell Separation Technology (Miltenyi Biotec). Chemotaxis of T cells was evaluated using 24-well migration chambers with 5-μm-pore-size inserts (Corning). Lower chambers were filled with 600 μl of the supernatants of lymphoma cells cultured with the indicated concentrations of tazemetostat or DMSO for 4 days (FL318) or 3 days (primary lymphoma cells), and 2×10^6 T cells were plated in the upper chambers and incubated at 37°C for 12 hours. In blocking experiments using the anti-CCR4 antibody, T cells were incubated for 1 hour with different concentrations of anti-CCR4 antibody (Cayman Chemical) before the cell migration assay. T cells that migrated from the upper to the lower chambers were collected, and the cell numbers were calculated using an MTT assay kit (Roche Diagnostics), and the T-cell subpopulation was analyzed by flow cytometry after migration.

2.8 | Flow cytometry

Flow cytometry was performed using a FACSLyric flow cytometer (BD Biosciences). Antibodies used for flow cytometry were as follows: anti-CD4-APC or anti-CD4-FITC (A161A1; BioLegend), anti-CD8-PE/Cy7-A (RPA-T8; BioLegend), anti-CD45RA-FITC (HI100; BioLegend), CD25-PE/Cy7-A (BC96; BioLegend), and anti-Human FOXP3 Staining Set PE (236A/E7, eBioscience). The $CD4^+CD25^+FoxP3^+$ population was classified into three subpopulations based on the expression levels of CD45RA and FoxP3, $CD45RA^+FoxP3^{low}$ resting Treg cells, $CD45RA^+FoxP3^{high}$ activated Treg cells, and $CD45RA^-FoxP3^{low}$ cytokine-secreting nonsuppressive cells,[25] and the sum of the former two cell groups was evaluated as total Treg cells.

2.9 | Interferon (IFN)-γ production assay of T cells

After the transwell migration assay, T cells were collected and seeded in a 96-well plate and cultured with 4 Gy-irradiated 1×10^5 cells/well of FL318, whose supernatants were used for cell migration. In the indicated samples, 5 μg/mL of anti-PD-1 antibody (nivolumab; Ono Pharmaceutical) were added. After culturing for 3 days, supernatants were examined for IFN-γ production by T cells using a human IFN-γ ELISA kit (BioLegend).

2.10 | Analysis of human lymphoma databases

The core dataset of DLBCL samples (278 GCB-DLBCL and 252 ABC-DLBCL samples) was obtained from EGA (dataset id: EGA00001003600),[26] and a dataset of 40 FL samples was obtained from International Cancer Genome Consortium (ICGC) Malignant Lymphoma–Germinal center B-cell–derived lymphomas project (https://icgc.org/icgc/cgp/64/345/53049).[27] Gene expression was measured using terms of fragments per kilobase of exon per million fragments mapped and normalized using the Cufflinks package, version 2.2.124. Quantile normalization was performed, and the data were log2 normalized. To evaluate the correlation between *CCL17* expression and the cell signatures of $CD4^+$ T cells, $CD8^+$ T cells, Treg cells, follicular dendritic cells, myeloid cells, and stromal cells,[28] the geometric mean (log-average) of the expression of genes was calculated. The EZH2-activated signature was determined as a reciprocal of the signature calculated from the gene set upregulated by GSK343 in a GCB-DLBCL cell line.[29] EZH2-activating mutations were defined as Y641F/N/S/H/C, A677G, and A687V.[30]

3 | RESULTS

3.1 | *CCR17* is upregulated by tazemetostat in B-cell lymphoma lines

In our previous analysis of microarray gene expression profiling of two human B-cell lymphoma lines, FL218 and DLBCL2, 89 genes were upregulated more than twofold in both cell lines after tazemetostat treatment.[31] To explore the potential treatment targets of the agent, we selected seven candidate genes known to be associated with B-cell differentiation and/or intercellular interaction (*CCL17*, *TNFRSF25*, *IL22RA1*, *ID2*, *BACH2*, *ITGAV*, *ID3*), and their changes in gene expression after tazemetostat treatment were evaluated in 11 B-cell lymphoma lines by qRT-PCR. Among these genes, we found that *CCL17* expression was significantly upregulated after tazemetostat treatment in all B-cell lymphoma lines tested, especially in those of germinal center B-cell origin (FL, GCB-DLBCL, BL) (Figure 1A, B).

CCL17 is a chemokine that is physiologically expressed in antigen-presenting cells such as dendritic cells,[13,14] and is well known to be a hallmark of H/RS cells in HL. As H/RS cells are considered to be originated from germinal center B cells,[32,33] we hypothesized that an EZH2 inhibitor may have a function of altering the gene expression pattern of B-cell lymphomas to those typical of H/RS cells. We compared gene expression profiling of five FL cell lines with and without tazemetostat treatment and three HL cell lines by RNA-seq, and found that tazemetostat treatment altered the gene expression of FL cell lines similar to that of HL cell lines (Figure 1C). Among 2589 genes expressed more than twofold in HL than in FL cell lines, 468 (18.1%) were upregulated more than twofold by tazemetostat in FL, whereas only 33 (1.3%) were downregulated less than 0.5-fold. On the other hand, among 1999 genes that were expressed less than 0.5-fold in HL than in FL cell lines, only six (0.3%) were upregulated more than twofold by tazemetostat in FL, whereas 76 genes (3.8%) were downregulated less than 0.5-fold.

We next performed GSEA for five FL cell lines with versus without tazemetostat treatment for 83 genes that were reported to be upregulated in H/RS cells microdissected from HL tissues.[12] Notably, a positive correlation was demonstrated between genes upregulated by tazemetostat in FL cell lines and H/RS cells (Figure 1D, Table 2). To examine whether this effect of tazemetostat is affected by the gene mutations in lymphoma cells, we evaluated mutations in 29 representative genes in FL[34] in the five FL cell lines based on the RNA-seq analysis. These FL cell lines carried mutations in 13 of the 29 genes examined, including those coding for different epigenetic modifiers, but only one (FL218) carried an EZH2-activating mutation (Figure 1E). According to these results, it is demonstrated that tazemetostat has a function of upregulating HL-related genes in FL cell lines, regardless of EZH2 mutations.

FIGURE 1 *CCL17* gene expression is enhanced in B-cell lymphoma lines by tazemetostat. A, Fold changes in the expression levels of seven candidate genes in B-cell lymphoma lines treated with tazemetostat (5 μM, 4 d). Gene expression levels were examined by qPCR and normalized to the expression level of *ACTB*. Fold changes in gene expression in cells treated with tazemetostat compared with DMSO-treated controls were calculated. B, Results of the changes in *CCL17* gene expression levels of B-cell lymphoma lines treated with tazemetostat (black bars) compared with DMSO-treated controls (gray bars). *CCL17* gene expression levels were examined by qPCR and normalized to the expression level of *ACTB*. The vertical bars indicate standard deviation of the duplicates. C, Gene expression alterations induced by tazemetostat treatment in 5 FL cell lines. Genes upregulated by tazemetostat were enriched in the genes that were expressed higher than 2-fold in Hodgkin lymphoma (HL) than in follicular lymphoma (FL) cell lines (upper panel), and genes downregulated by tazemetostat were enriched in the genes that were expressed lower than 0.5-fold in HL than in FL cell lines (lower panel). D, Gene set enrichment analysis (GSEA) enrichment plot for five FL cell lines with versus without tazemetostat treatment for genes reported to be upregulated in Hodgkin/Reed-Sternberg (H/RS) cells microdissected from HL tissues.[12] E, Representative gene mutations in five FL cell lines. All of them are positive for t(14;18) translocation[15]

(A)

	FL					DLBCL			BL		MCL
	FL18	FL218	FL318	FL518	FL618	DLBCL2	SUDHL6	HBL-1	Raji	Daudi	Granta519
CCL17	94.8	116.5	51.7	>50	11.7	1.8	55.1	18.8	16.3	>50	1.8
TNFRSF25	3.5	2.8	2.1	0.3	4.4	1.4	7.3	5.4	10.2	>50	6.6
IL22RA1	2.9	16.9	2.1	1.6	2.8	1.6	0.58	2.3	7	3.7	2.4
ID2	1.2	9.8	1.1	0.65	2.7	1.39	0.99	2.3	1.5	3.4	3.4
BACH2	1.2	7.7	0.3	0.3	1.4	4.2	1.5	0.4	1.2	0.7	2.7
ITGAV	0.99	3.7	1.4	0.4	1.7	1.6	2.2	1.7	2.8	1.4	0.7
ID3	0.97	3.1	0.8	7.4	1.5	3.4	0.7	6.6	0.8	0.5	2.2

>50 fold
10-50 fold
2-10 fold
1-2 fold
0.5-1 fold
<0.5 fold

(B)

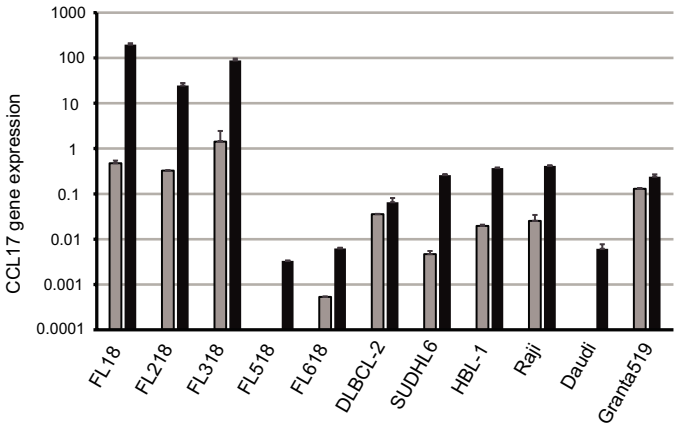

(C)

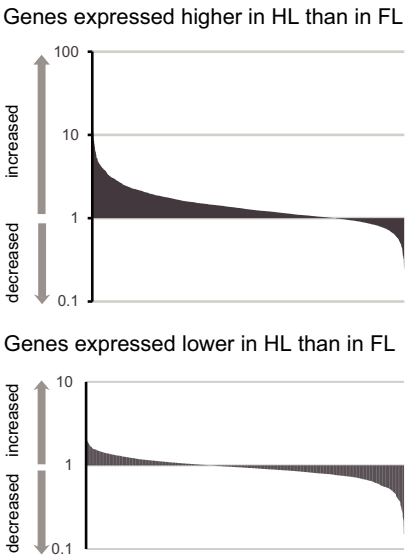

(D)

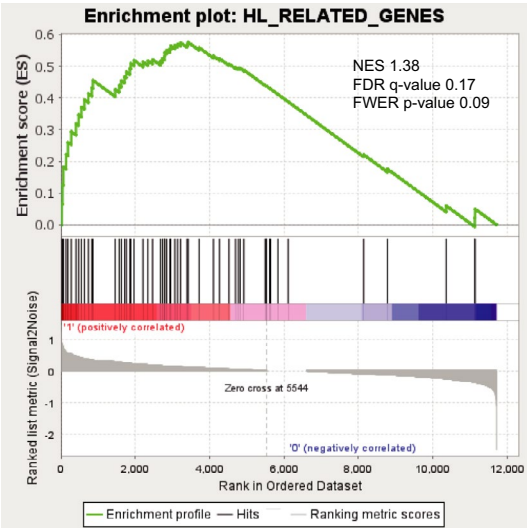

(E)

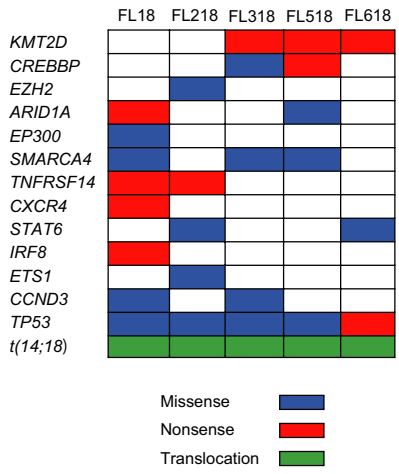

TABLE 2 Gene set enrichment analysis (GSEA) details

	Rank metric score	Running ES	Core enrichment
ADRB2	0.882	0.0661	Yes
PCGF2	0.802	0.1264	Yes
CXCL10	0.747	0.1819	Yes
LMNA	0.601	0.222	Yes
IL6	0.548	0.26	Yes
PTPRG	0.535	0.2938	Yes
SERPINA1	0.467	0.3189	Yes
CCL22	0.436	0.3465	Yes
STAT1	0.403	0.3712	Yes
AMPH	0.389	0.3943	Yes
WT1	0.365	0.4134	Yes
SOCS3	0.343	0.4319	Yes
RTN1	0.339	0.4558	Yes
MT2A	0.294	0.427	Yes
TNFRSF11A	0.275	0.4392	Yes
CD44	0.268	0.455	Yes
IER3	0.256	0.4671	Yes
STAT5A	0.25	0.4824	Yes
CCND2	0.238	0.4927	Yes
PRAME	0.235	0.509	Yes
SOCS2	0.224	0.5185	Yes
MUC1	0.201	0.5133	Yes
ATF3	0.196	0.5173	Yes
JUN	0.186	0.521	Yes
FBXO32	0.169	0.5158	Yes
ID2	0.164	0.5241	Yes
RASSF4	0.159	0.5317	Yes
CX3CL1	0.157	0.5432	Yes
GJB2	0.153	0.5505	Yes
TNFAIP6	0.149	0.5548	Yes
CCL17	0.149	0.5642	Yes
GNA15	0.143	0.5662	Yes
HGF	0.139	0.5705	Yes
CCL5	0.135	0.5741	Yes
FOXC1	0.123	0.5686	Yes
PHLDA1	0.121	0.5756	Yes

3.2 | Tazemetostat enhances *CCL17* promoter activity by EZH2 inhibition leading to demethylation of H3K27me3

EZH2 functions as a transcriptional repressor by catalyzing histone H3K27 trimethylation[35]; therefore, we hypothesized that the *CCL17* promoter region is enriched in repressive histone modification H3K27me3, and tazemetostat induces *CCL17* gene expression by inhibiting EZH2 and leading to H3K27 demethylation of the promoter. We performed ChIP of FL318 cells with an anti-H3K27me3 antibody and quantified the *CCL17* promoter region in the precipitated samples by qPCR. We found that the *CCL17* promoter region was more highly marked with H3K27me3 in FL318, and treatment of the cells with tazemetostat led to its reduction (Figure 2A). These results indicated that *CCL17* promoter activity is repressed by H3K27me3, and tazemetostat is able to reverse this epigenetic repression by inhibiting the function of EZH2.

As tazemetostat upregulated the gene expression of FL cells more similar to H/RS cells, we hypothesized that different epigenetic regulation partly determines the difference in FL and HL gene expression. Chromosome band 9p24 is reported to be frequently amplified in HL cells, and histone demethylase KDM4C/JMJD2C is identified as an oncogene in this amplicon.[36] We found that knockdown of *KDM4C* in two HL cell lines, L428 and HDLM2, downregulated the expression of *CCL17* (Figure 2B). According to these findings, it is suggested that the gene expressions of FL and HL cells are partly reciprocally regulated by the histone modifications, and alterations in epigenetic regulation can reverse these gene expressions.

3.3 | Tazemetostat enhances CCL17 secretion in B-cell lymphoma lines

CCL17 is a chemokine that is physiologically produced by antigen-presenting cells and leads to the activation and migration of T cells expressing its receptor CCR4. To evaluate whether tazemetostat treatment enhances CCL17 production in B-cell lymphomas, we examined CCL17 levels in the supernatant of the representative four B-cell lymphoma lines cultured with or without tazemetostat. We found that CCL17 levels were increased in FL18, FL318, and Raji cells in parallel with the concentration of tazemetostat, and costimulation with CpG further enhanced its production (Figure 3). In SUDHL6, CCL17 was not produced solely by tazemetostat, but concurrent treatment with CpG induced CCL17 secretion.

3.4 | CCL17 produced by B-cell lymphoma cells enhances migration of T cells with potential cytotoxic activity

We next performed an in vitro transwell T-cell migration assay to examine whether enhancement of CCL17 production in B-cell lymphoma with tazemetostat treatment can promote chemotaxis of T cells. T cells of healthy donors were placed in the upper chambers of the transwell culture plate, and the lower chambers were filled with a supernatant of FL318 cells cultured in conditions with various tazemetostat concentrations. After culturing T cells for 12 hours, the number of T cells that migrated to the lower chambers was calculated. We found that the number of T cells that

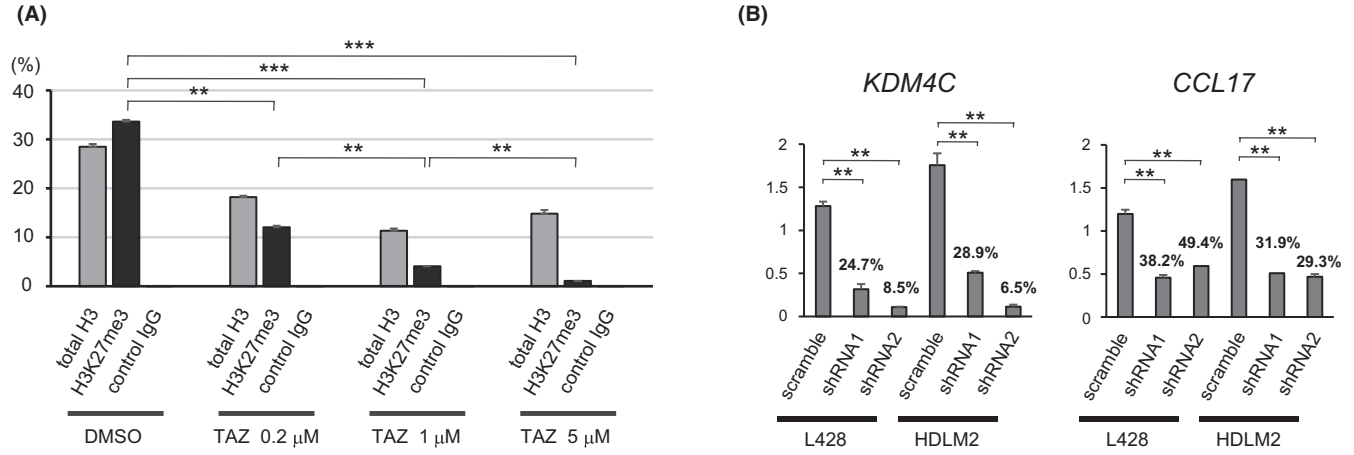

FIGURE 2 Epigenetic regulation of *CCL17* gene. A, FL318 cells with or without tazemetostat treatment were subjected to chromatin immunoprecipitation (ChIP) using anti-total H3 (gray bars), anti-H3K27me3 (black bars), and control IgG antibodies (white bars), followed by qPCR of the *CCL17* promoter region. The amounts of precipitated DNA relative to the input are demonstrated. The vertical bars indicate standard deviation of the duplicates (**$P < .01$, ***$P < .001$; Student's *t*-test). B, *KDM4C* was knocked down in two Hodgkin lymphoma (HL) cell lines, L428 and HDLM2, by two different *KDM4C* shRNA constructs. *KDM4C* and *CCL17* expression levels were evaluated by qPCR and normalized to the expression level of *ACTB*. The vertical bars indicate standard deviation of the duplicates (**$P < .01$; Student's *t*-test)

migrated increased when the lower chamber was filled with supernatant from FL318 cells treated with higher tazemetostat concentrations (Figure 4A). In contrast, cell migration was suppressed when T cells were pretreated with CCR4-blocking antibody, indicating that T-cell migration was mainly driven by CCL17 produced by FL318 cells. Moreover, we were able to detect CCL17 secretion from in vitro–cultured primary B-cell lymphoma cells in parallel with the concentration of tazemetostat, and CCL17 secreted by primary lymphoma cells similarly had the function of inducing T cell migration (Figure 4B).

Evaluation of migrated $CD4^+$, $CD8^+$, and Treg-cell subsets using an MTT assay and flow cytometry demonstrated that although CCR4 is typically expressed on Treg cells, migrated cells contained much larger numbers of nonregulatory $CD4^+$ and $CD8^+$ T cells than Treg cells (Figure 4C). These results indicated that CCL17 produced by lymphoma cells has a function of attracting not only Treg cells but also broader T cell subsets.

CCL17 expressed in H/RS cells is known to be strongly associated with T-cell–rich microenvironment of HL. As PD-1 blockade therapy is recognized as a highly effective treatment for HL,[37-39] we hypothesized that PD-1 blockade may be able to similarly enhance the antilymphoma immune response of T cells attracted to CCL17 secreted by B-cell lymphoma. To solve this question, we cultured FL318 cells with T cells that migrated toward the supernatant of FL318 cells treated with or without tazemetostat. We found that T cells that migrated toward the supernatant of FL318 cells treated with tazemetostat produced higher levels of IFN-γ against FL318, and IFN-γ production was further enhanced when PD-1 blocking antibody was added (Figure 4D). These results suggested that T cells attracted to CCL17 produced by B-cell lymphoma can exert cytotoxicity against lymphoma cells, and the reaction is further enhanced by PD-1 blockade.

3.5 | CCL17 expression parallels the T-cell–rich microenvironment in human B-cell lymphomas

Our observation that an EZH2 inhibitor has a function of inducing CCL17 secretion by B-cell lymphoma cell lines led us to question whether CCL17 can be expressed and involved in the regulation of immune microenvironment in human B-cell lymphomas. We analyzed publicly available FL and DLBCL databases to elucidate the relationship of EZH2 activity, *CCL17* expression, and T-cell signatures in human B-cell lymphoma samples.[26,27] In the FL and GCB-DLBCL datasets, EZH2-activating mutations (Y641F/N/S/H/C, A677G, and A687V)[30] were found in six out of 40 FL samples and 35 out of 278 GCB-DLBCL samples, and these samples presented with a higher EZH2-activated signature[29] and lower *CCL17* gene expression (Figure 5A). In ABC-DLBCL, on the other hand, the number of samples with EZH2-activating mutations was too small to analyze (three out of 252 samples). We further found that *CCL17* expression levels were significantly inversely correlated with a high EZH2-activated signature in FL and GCB-DLBCL but not in ABC-DLBCL (Figure 5B). Notably, *CCL17* expression levels were significantly associated with not only the Treg cell signature but also $CD4^+$ and $CD8^+$ T-cell signatures in FL and GCB-DLBCL (Figure 5B). On the other hand, *CCL17* expression has no or weaker association with other cell signatures such as follicular dendritic cells, myeloid cells, or stromal cells (Figure S1). These results were considered to correspond well with our findings that CCL17 produced by B-cell lymphoma induces T-cell chemotaxis and promotes a T-cell–rich tumor microenvironment.

4 | DISCUSSION

Epigenetic modification regulates the transcription of many genes, plays critical roles in cell development and differentiation, and is also

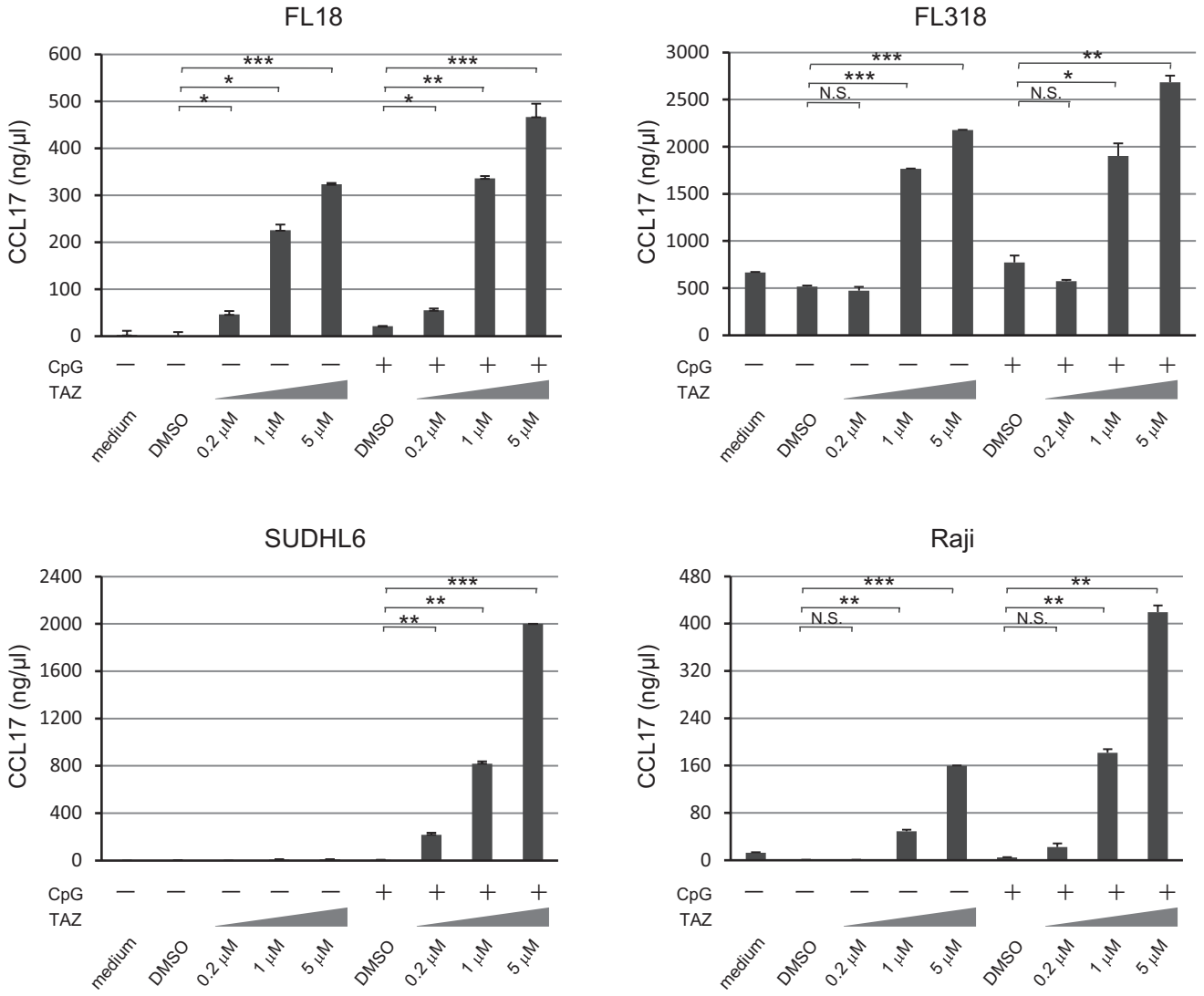

FIGURE 3 CCL17 secretion is induced by tazemetostat in B-cell lymphoma lines. B-cell lymphoma lines (FL18, FL318, SUDHL6, Raji) were cultured with tazemetostat at the indicated concentration (0.2, 1, and 5 μM) or DMSO for 4 d, with or without 1 μM CpG stimulation for the last 1 d. Cell supernatants were then collected and examined for CCL17 protein levels by ELISA. The vertical bars indicate standard deviation of the duplicates (*$P < .05$, **$P < .01$; ***$P < .001$; NS, not significant; Student's *t*-test)

FIGURE 4 CCL17 secreted from B-cell lymphoma cells enhances T cell migration. A, Chemotaxis of T cells was evaluated using a chamber plate separated with 5-μm-pore inserts. Peripheral T cells from healthy donors were plated in the upper chambers, and after a 12-h incubation, T cells that migrated to the bottom chambers were quantified using an MTT assay. In the indicated samples, T cells were incubated for 1 h with an anti-CCR4 antibody before plating for migration. Results from two different T-cell donors are shown. The vertical bars indicate standard deviation of the duplicates (*$P < .05$; **$P < .01$; NS, not significant; Student's *t*-test). B, Primary B-cell lymphoma cells were cultured with CD40L-transfected L cells and tazemetostat at the indicated concentration, and cell supernatants were examined for CCL17 by ELISA (left panel). Chemotaxis of T cells toward CCL17 secreted from primary B-cell lymphoma cells was evaluated with the same method as in Figure 4A (right panel). In the indicated samples, T cells were preincubated for 1 h with an anti-CCR4 antibody. The vertical bars indicate standard deviation of the duplicates (**$P < .01$; ***$P < .001$; NS, not significant; Student's *t*-test). C, Cell numbers of the T-cell subsets migrated toward the supernatant of FL318 treated with DMSO or tazemetostat (5 μM). Mean of the data from two different T-cell donors are shown (*$P < .05$; **$P < .01$; ***$P < .001$; Student's *t*-test). D, Interferon (IFN)-γ production of T cells that migrated toward the CCL17-expressing B-cell lymphoma line. T cells that migrated toward the supernatant of FL318 treated with DMSO or tazemetostat (5 μM) were cultured with FL318. In the indicated wells, anti-PD-1 antibody was added. After culturing for 3 d, supernatants were examined for IFN-γ production by T cells by ELISA. Mean of the data from two different T-cell donors are shown (*$P < .05$; **$P < .01$; NS, not significant; Student's *t*-test)

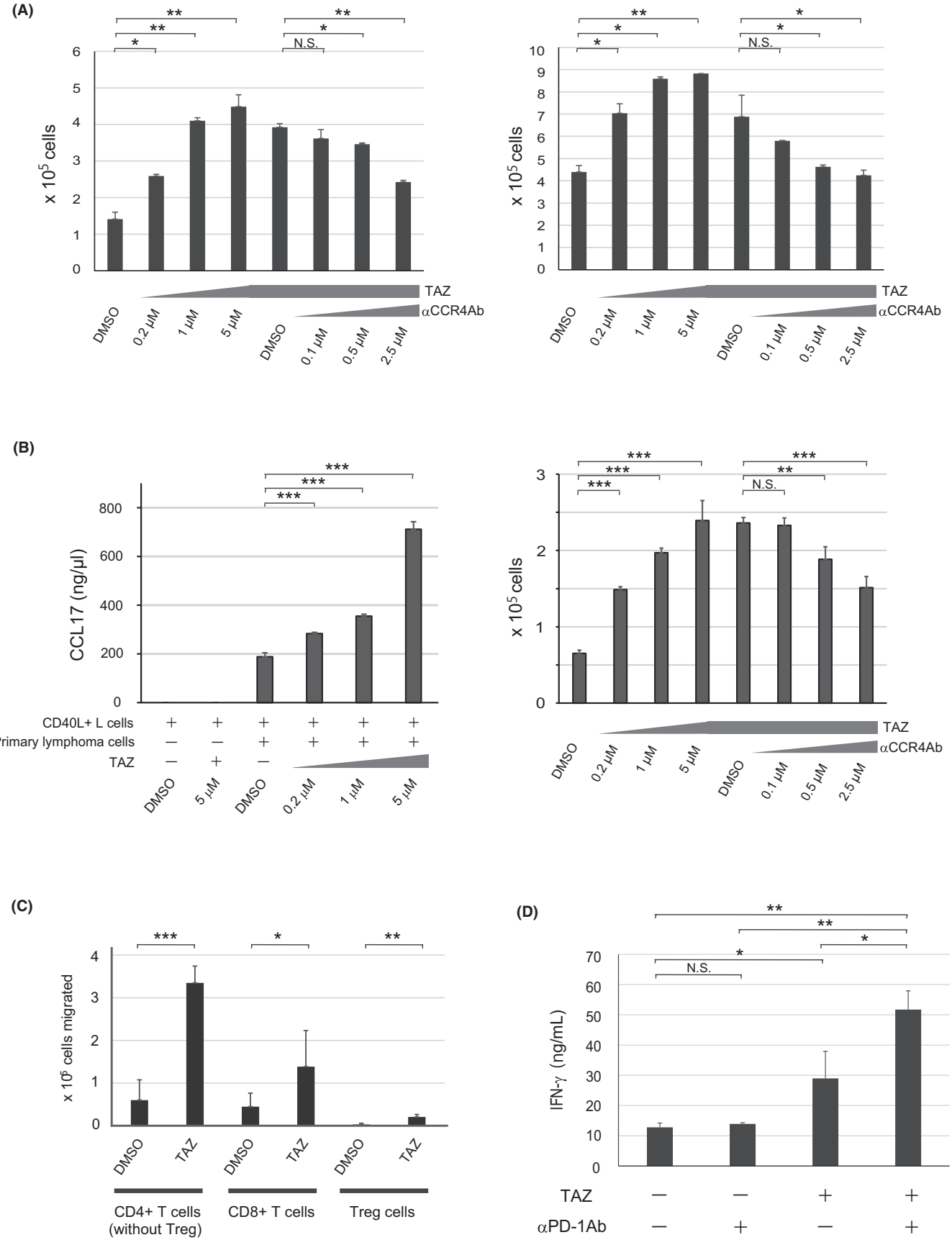

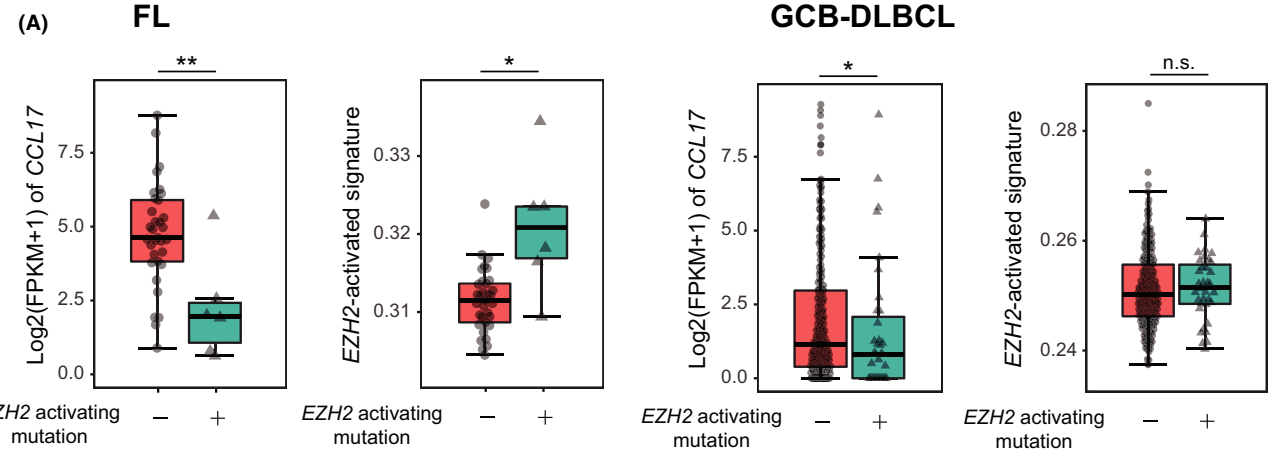

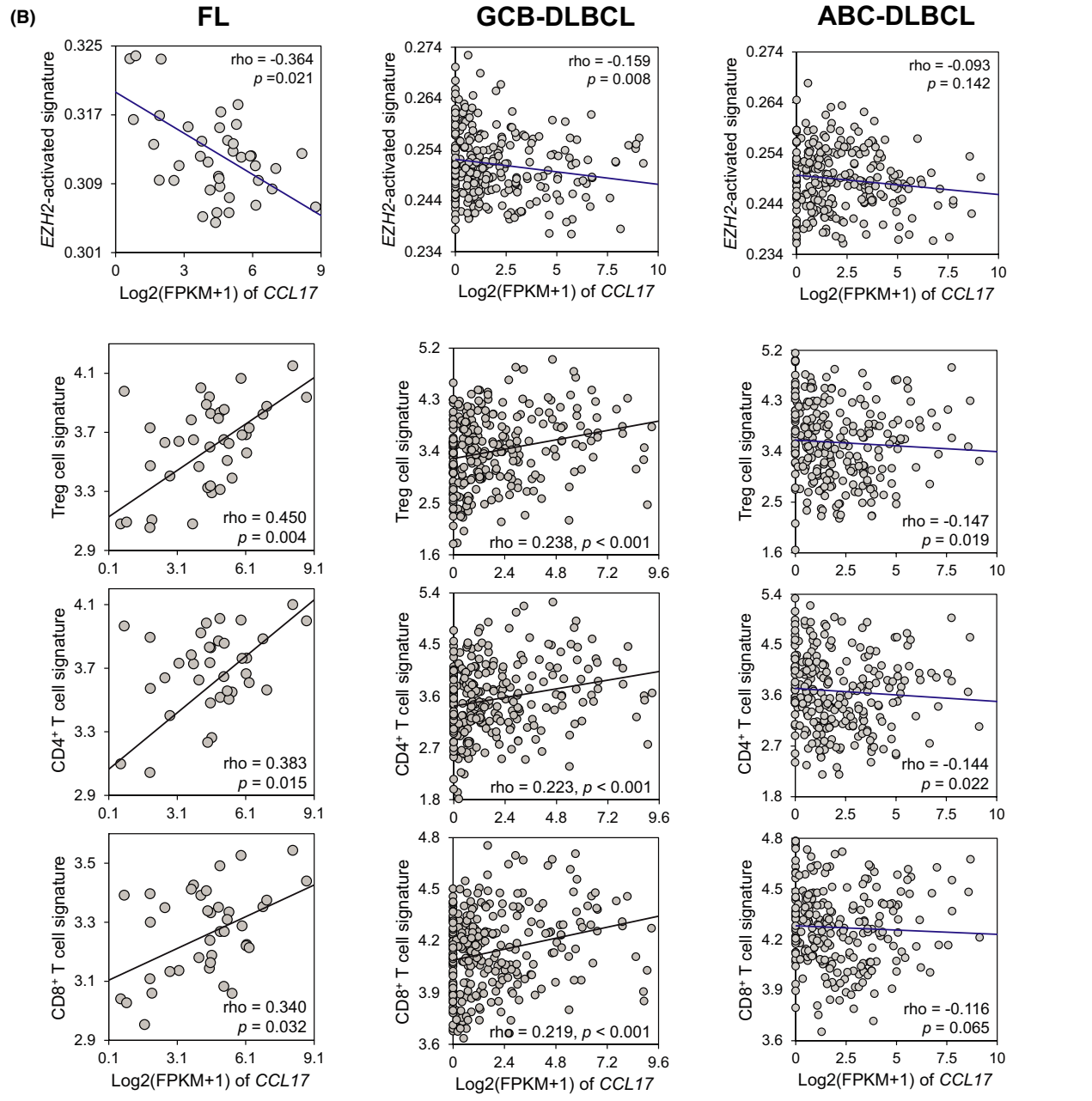

FIGURE 5 *CCL17* expression level is inversely correlated with high EZH2-activated signature and parallels T-cell signatures in follicular lymphoma (FL) and germinal center B-cell–like diffuse large B-cell lymphoma (GCB-DLBCL). A, Relationship between *CCL17* expression, presence of EZH2-activating mutations, and EZH2-activated signature was analyzed in 40 FL[27] (left panels) and 278 GCB-DLBCL[26] samples (right panels). Six of the 40 FL and 35 of the 278 GCB-DLBCL samples were positive for EZH2-activating mutations. The data were analyzed statistically using *t*-test (FL) and Steel's test (GCB-DLBCL; ** $P < .01$, *$P < .05$). B, *CCL17* expression was significantly associated with Treg, $CD4^+$, and $CD8^+$ T-cell signatures in FL (left panels) and GCB-DLBCL (middle panels), but not activated B-cell–like (ABC)-DLBCL (right panels). The geometric mean (log-average) of the expression of genes was calculated, and the correlation of *CCL17* expression and each T-cell signature was investigated using Spearman's correlation coefficient

involved in the pathogenesis of a variety of malignancies. In this report, we have demonstrated that the EZH2 inhibitor tazemetostat leads to *CCL17* upregulation in B-cell lymphomas.

CCL17 is typically overexpressed in H/RS cells and is responsible for the T-cell–rich microenvironment of HL.[11,40] In addition to *CCL17*, we have found a positive correlation between genes upregulated by tazemetostat in five FL cell lines and those reported to be overexpressed in H/RS cells microdissected from HL tissues.[12] The *CCL17* promoter region is found to be enriched in H3K27me3, and EZH2 inhibition induces its demethylation and activates *CCL17* gene transcription. On the other hand, knockdown of *KDM4C* in HL cell lines is shown to downregulate *CCL17* expression. According to these findings, it is suggested that the gene expressions of FL and HL cells are partly reciprocally regulated by histone modifications, and alterations in epigenetic regulation can reverse these gene expressions. It is clinically recognized that, in some rare instances, lymphoma patients develop two distinct types of lymphoma called composite lymphomas, and many of the composite cases with HL and B-cell lymphoma are clonally related.[41-49] Based on our findings, it can be speculated that HL and B-cell lymphoma may evolve concurrently from the same lymphoma clone when two different epigenetic modifications occur during the developmental process.

We have also shown that enhanced secretion of CCL17 from B-cell lymphoma cells by tazemetostat promoted the recruitment and IFN-γ secretion of T cells against lymphoma cells, and the addition of anti-PD-1 antibody further enhanced the IFN-γ secretion of T cells that migrated toward CCL17. Finally, we analyzed human lymphoma databases and found that the *CCL17* expression level inversely paralleled the EZH2 activation signature and significantly paralleled the T-cell–rich microenvironment in FL and GCB-DLBCL.

The high efficacy of PD-1 blockade therapy in HL has been demonstrated in several clinical studies[37-39] and in clinical practices. In contrast, B-cell malignancies are less sensitive to PD-1 blockade therapy,[50,51] which could be partly explained by the scarcity of tumor-infiltrating T cells that can readily exert antitumor immune responses.[52-54] Our findings suggest that an EZH2 inhibitor can induce T-cell inflamed lymphoma microenvironment and is expected to be utilized for amplifying the effect of immunotherapy.

We observed *CCL17* upregulation by tazemetostat in all 11 B-cell lymphoma lines tested, irrespective of their histologic origin. In the analysis of FL and GCB-DLBCL databases, *CCL17* expression levels were shown to significantly inversely parallel the EZH2-activated signature and positively correlate with both $CD4^+$ and $CD8^+$ T-cell signatures. On the other hand, the association among *CCL17* expression levels, EZH2-activated signature, and T-cell signatures was unclear in ABC-DLBCL samples. Although we do not have any clear explanation, there may be additional factors that affect the extent of tumor-infiltrating T cells in ABC-DLBCL. As our findings are mainly based on the experiment of cell lines, further analysis is necessary to find out whether the EZH2 inhibitor actually has a function in upregulating CCL17 and increasing tumor-infiltrating T cells in B-cell lymphoma patients.

In summary, we found that the EZH2 inhibitor tazemetostat upregulates *CCL17* expression in B-cell lymphoma cells and facilitates T-cell recruitment, which have the potential to exert antilymphoma responses. We propose that EZH2 inhibition in B-cell lymphomas promotes T-cell infiltration into the tumor microenvironment. Although further studies are warranted, our findings provide a rationale for the combination of an EZH2 inhibitor with immunotherapy.

ACKNOWLEDGMENTS

This work was supported by the Japan Society for the Promotion of Science Grant Numbers 15K09474 and 18K08324 (MN). The authors would like to thank A. Reddy and S. S. Dave (Duke University, Durham, NC) for kindly providing access to the DLBCL database.

CONFLICT OF INTEREST

M. Nishikori and A. Takaori-Kondo have received honoraria and research funding from Eisai Co., Ltd. The other authors have no financial conflicts of interest related to the preparation and publication of this article.

ORCID

Momoko Nishikori https://orcid.org/0000-0003-4171-2162
Toshio Kitawaki https://orcid.org/0000-0002-6373-3442

REFERENCES

1. Morin RD, Johnson NA, Severson TM, et al. Somatic mutations altering EZH2 (Tyr641) in follicular and diffuse large B-cell lymphomas of germinal-center origin. *Nat Genet*. 2010;42(2):181-185.
2. Bodor C, O'Riain C, Wrench D, et al. EZH2 Y641 mutations in follicular lymphoma. *Leukemia*. 2011;25(4):726-729.
3. Ryan RJ, Nitta M, Borger D, et al. EZH2 codon 641 mutations are common in BCL2-rearranged germinal center B cell lymphomas. *PLoS One*. 2011;6(12):e28585.
4. Visser HP, Gunster MJ, Kluin-Nelemans HC, et al. The Polycomb group protein EZH2 is upregulated in proliferating, cultured human mantle cell lymphoma. *Br J Haematol*. 2001;112(4):950-958.
5. Zhang X, Zhao X, Fiskus W, et al. Coordinated silencing of MYC-mediated miR-29 by HDAC3 and EZH2 as a therapeutic target of histone modification in aggressive B-Cell lymphomas. *Cancer Cell*. 2012;22(4):506-523.

6. Knutson SK, Wigle TJ, Warholic NM, et al. A selective inhibitor of EZH2 blocks H3K27 methylation and kills mutant lymphoma cells. *Nat Chem Biol*. 2012;8(11):890-896.
7. McCabe MT, Ott HM, Ganji G, et al. EZH2 inhibition as a therapeutic strategy for lymphoma with EZH2-activating mutations. *Nature*. 2012;492(7427):108-112.
8. Italiano A, Soria JC, Toulmonde M, et al. Tazemetostat, an EZH2 inhibitor, in relapsed or refractory B-cell non-Hodgkin lymphoma and advanced solid tumours: a first-in-human, open-label, phase 1 study. *Lancet Oncol*. 2018;19(5):649-659.
9. Morschhauser F, Tilly H, Chaidos A, et al. Tazemetostat for patients with relapsed or refractory follicular lymphoma: an open-label, single-arm, multicentre, phase 2 trial. *Lancet Oncol*. 2020;21(11):1433-1442.
10. Munakata W, Shirasugi Y, Tobinai K, et al. Phase 1 study of tazemetostat in Japanese patients with relapsed or refractory B-cell lymphoma. *Cancer Sci*. 2021;112(3):1123-1131.
11. Kuppers R. The biology of Hodgkin's lymphoma. *Nat Rev Cancer*. 2009;9(1):15-27.
12. Steidl C, Diepstra A, Lee T, et al. Gene expression profiling of microdissected Hodgkin Reed-Sternberg cells correlates with treatment outcome in classical Hodgkin lymphoma. *Blood*. 2012;120(17):3530-3540.
13. Ono SJ, Nakamura T, Miyazaki D, Ohbayashi M, Dawson M, Toda M. Chemokines: roles in leukocyte development, trafficking, and effector function. *J Allergy Clin Immunol*. 2003;111(6):1185-1199. quiz 200.
14. Kupper TS, Fuhlbrigge RC. Immune surveillance in the skin: mechanisms and clinical consequences. *Nat Rev Immunol*. 2004;4(3):211-222.
15. Maesako Y, Uchiyama T, Ohno H. Comparison of gene expression profiles of lymphoma cell lines from transformed follicular lymphoma, Burkitt's lymphoma and de novo diffuse large B-cell lymphoma. *Cancer Sci*. 2003;94(9):774-781.
16. Epstein AL, Levy R, Kim H, Henle W, Henle G, Kaplan HS. Biology of the human malignant lymphomas. IV. Functional characterization of ten diffuse histiocytic lymphoma cell lines. *Cancer*. 1978;42(5):2379-2391.
17. Nozawa Y, Abe M, Wakasa H, et al. Establishment and characterization of an Epstein-Barr virus negative B-cell lymphoma cell line and successful heterotransplantation. *Tohoku J Exp Med*. 1988;156(4):319-330.
18. Pulvertaft JV. Cytology of Burkitt's tumour (African Lymphoma). *Lancet*. 1964;1(7327):238-240.
19. Klein E, Klein G, Nadkarni JS, Nadkarni JJ, Wigzell H, Clifford P. Surface IgM-kappa specificity on a Burkitt lymphoma cell in vivo and in derived culture lines. *Cancer Res*. 1968;28(7):1300-1310.
20. Jadayel DM, Lukas J, Nacheva E, et al. Potential role for concurrent abnormalities of the cyclin D1, p16CDKN2 and p15CDKN2B genes in certain B cell non-Hodgkin's lymphomas. Functional studies in a cell line (Granta 519). *Leukemia*. 1997;11(1):64-72.
21. Nishikori M, Maesako Y, Ueda C, Kurata M, Uchiyama T, Ohno H. High-level expression of BCL3 differentiates t(2;5)(p23;q35)-positive anaplastic large cell lymphoma from Hodgkin disease. *Blood*. 2003;101(7):2789-2796.
22. Kadowaki N, Ho S, Antonenko S, et al. Subsets of human dendritic cell precursors express different toll-like receptors and respond to different microbial antigens. *J Exp Med*. 2001;194(6):863-869.
23. Subramanian A, Tamayo P, Mootha VK, et al. Gene set enrichment analysis: a knowledge-based approach for interpreting genome-wide expression profiles. *Proc Natl Acad Sci USA*. 2005;102(43):15545-15550.
24. Lee TI, Johnstone SE, Young RA. Chromatin immunoprecipitation and microarray-based analysis of protein location. *Nat Protoc*. 2006;1(2):729-748.
25. Miyara M, Yoshioka Y, Kitoh A, et al. Functional delineation and differentiation dynamics of human CD4+ T cells expressing the FoxP3 transcription factor. *Immunity*. 2009;30(6):899-911.
26. Reddy A, Zhang J, Davis NS, et al. Genetic and functional drivers of diffuse large B cell lymphoma. *Cell*. 2017;171(2):481-94 e15.
27. Richter J, Schlesner M, Hoffmann S, et al. Recurrent mutation of the ID3 gene in Burkitt lymphoma identified by integrated genome, exome and transcriptome sequencing. *Nat Genet*. 2012;44(12):1316-1320.
28. Shaffer AL, Wright G, Yang L, et al. A library of gene expression signatures to illuminate normal and pathological lymphoid biology. *Immunol Rev*. 2006;210:67-85.
29. Beguelin W, Popovic R, Teater M, et al. EZH2 is required for germinal center formation and somatic EZH2 mutations promote lymphoid transformation. *Cancer Cell*. 2013;23(5):677-692.
30. Ott HM, Graves AP, Pappalardi MB, et al. A687V EZH2 is a driver of histone H3 lysine 27 (H3K27) hypertrimethylation. *Mol Cancer Ther*. 2014;13(12):3062-3073.
31. Otsuka Y, Nishikori M, Arima H, et al. EZH2 inhibitors restore epigenetically silenced CD58 expression in B-cell lymphomas. *Mol Immunol*. 2020;119:35-45.
32. Kanzler H, Küppers R, Hansmann ML, Rajewsky K. Hodgkin and Reed-Sternberg cells in Hodgkin's disease represent the outgrowth of a dominant tumor clone derived from (crippled) germinal center B cells. *J Exp Med*. 1996;184(4):1495-1505.
33. Marafioti T, Hummel M, Foss HD, et al. Hodgkin and reed-sternberg cells represent an expansion of a single clone originating from a germinal center B-cell with functional immunoglobulin gene rearrangements but defective immunoglobulin transcription. *Blood*. 2000;95(4):1443-1450.
34. Pastore A, Jurinovic V, Kridel R, et al. Integration of gene mutations in risk prognostication for patients receiving first-line immunochemotherapy for follicular lymphoma: a retrospective analysis of a prospective clinical trial and validation in a population-based registry. *Lancet Oncol*. 2015;16(9):1111-1122.
35. Bracken AP, Helin K. Polycomb group proteins: navigators of lineage pathways led astray in cancer. *Nat Rev Cancer*. 2009;9(11):773-784.
36. Rui L, Emre NC, Kruhlak MJ, et al. Cooperative epigenetic modulation by cancer amplicon genes. *Cancer Cell*. 2010;18(6):590-605.
37. Ansell SM, Lesokhin AM, Borrello I, et al. PD-1 blockade with nivolumab in relapsed or refractory Hodgkin's lymphoma. *N Engl J Med*. 2015;372(4):311-319.
38. Armand P, Engert A, Younes A, et al. Nivolumab for relapsed/refractory classic hodgkin lymphoma after failure of autologous hematopoietic cell transplantation: extended follow-up of the multicohort single-arm phase II CheckMate 205 trial. *J Clin Oncol*. 2018;36(14):1428-1439.
39. Chen R, Zinzani PL, Fanale MA, et al. Phase II study of the efficacy and safety of pembrolizumab for relapsed/refractory classic Hodgkin lymphoma. *J Clin Oncol*. 2017;35(19):2125-2132.
40. Steidl C, Connors JM, Gascoyne RD. Molecular pathogenesis of Hodgkin's lymphoma: increasing evidence of the importance of the microenvironment. *J Clin Oncol*. 2011;29(14):1812-1826.
41. Yoshida M, Ichikawa A, Miyoshi H, et al. High frequency of t(14;18) in Hodgkin's lymphoma associated with follicular lymphoma. *Pathol Int*. 2012;62(8):518-524.
42. Küppers R, Dührsen U, Hansmann ML. Pathogenesis, diagnosis, and treatment of composite lymphomas. *Lancet Oncol*. 2014;15(10):e435-e446.
43. Bräuninger A, Hansmann ML, Strickler JG, et al. Identification of common germinal-center B-cell precursors in two patients with both Hodgkin's disease and non-Hodgkin's lymphoma. *N Engl J Med*. 1999;340(16):1239-1247.

44. Huang Q, Wilczynski SP, Chang KL, Weiss LM. Composite recurrent hodgkin lymphoma and diffuse large B-cell lymphoma: one clone, two faces. *Am J Clin Pathol*. 2006;126(2):222-229.
45. Küppers R, Sousa AB, Baur AS, Strickler JG, Rajewsky K, Hansmann ML. Common germinal-center B-cell origin of the malignant cells in two composite lymphomas, involving classical Hodgkin's disease and either follicular lymphoma or B-CLL. *Mol Med*. 2001;7(5):285-292.
46. Marafioti T, Hummel M, Anagnostopoulos I, Foss HD, Huhn D, Stein H. Classical Hodgkin's disease and follicular lymphoma originating from the same germinal center B cell. *J Clin Oncol*. 1999;17(12):3804-3809.
47. Nakamura N, Ohshima K, Abe M, Osamura Y. Demonstration of chimeric DNA of bcl-2 and immunoglobulin heavy chain in follicular lymphoma and subsequent Hodgkin lymphoma from the same patient. *J Clin Exp Hematop*. 2007;47(1):9-13.
48. Rosenquist R, Roos G, Erlanson M, Küppers R, Bräuninger A, Hansmann ML. Clonally related splenic marginal zone lymphoma and Hodgkin lymphoma with unmutated V gene rearrangements and a 15-yr time gap between diagnoses. *Eur J Haematol*. 2004;73(3):210-214.
49. van den Berg A, Maggio E, Rust R, Kooistra K, Diepstra A, Poppema S. Clonal relation in a case of CLL, ALCL, and Hodgkin composite lymphoma. *Blood*. 2002;100(4):1425-1429.
50. Ansell SM, Minnema MC, Johnson P, et al. Nivolumab for relapsed/refractory diffuse large B-cell lymphoma in patients ineligible for or having failed autologous transplantation: a single-arm. Phase II Study. *J Clin Oncol*. 2019;37(6):481-489.
51. Lesokhin AM, Ansell SM, Armand P, et al. Nivolumab in patients with relapsed or refractory hematologic malignancy: preliminary results of a phase Ib study. *J Clin Oncol*. 2016;34(23):2698-2704.
52. Tumeh PC, Harview CL, Yearley JH, et al. PD-1 blockade induces responses by inhibiting adaptive immune resistance. *Nature*. 2014;515(7528):568-571.
53. Chen PL, Roh W, Reuben A, et al. Analysis of immune signatures in longitudinal tumor samples yields insight into biomarkers of response and mechanisms of resistance to immune checkpoint blockade. *Cancer Discov*. 2016;6(8):827-837.
54. Salmon H, Remark R, Gnjatic S, Merad M. Host tissue determinants of tumour immunity. *Nat Rev Cancer*. 2019;19(4):215-227.

SUPPORTING INFORMATION

Additional supporting information may be found online in the Supporting Information section.

How to cite this article: Yuan H, Nishikori M, Otsuka Y, Arima H, Kitawaki T, Takaori-Kondo A. The EZH2 inhibitor tazemetostat upregulates the expression of CCL17/TARC in B-cell lymphoma and enhances T-cell recruitment. *Cancer Sci*. 2021;112:4604–4616. https://doi.org/10.1111/cas.15122